Nuclear Instruments and Methods in Physics Research B 393 (2017) 144–149

Contents lists available at ScienceDirect

Nuclear Instruments and Methods in Physics Research B

journal homepage: www.elsevier.com/locate/nimb

First-principles investigation of the energetics of point defects at a grain boundary in tungsten

Jun Chai, Yu-Hao Li, Liang-Liang Niu, Shi-Yao Qin, Hong-Bo Zhou *, Shuo Jin, Ying Zhang, Guang-Hong Lu

Department of Physics, Beihang University, Beijing 100191, China
Beijing Key Laboratory of Advanced Nuclear Materials and Physics, Beihang University, Beijing 100191, China

ARTICLE INFO

Article history:
Received 20 July 2016
Received in revised form 28 November 2016
Accepted 29 November 2016
Available online 9 December 2016

Keywords:
Tungsten
Grain boundary
Point defects
First-principles

ABSTRACT

Tungsten (W) and W alloys are considered as the most promising candidates for plasma facing materials in future fusion reactor. Grain boundaries (GBs) play an important role in the self-healing of irradiation defects in W. Here, we investigate the stability of point defects [vacancy and self-interstitial atoms (SIA's)] in a $\Sigma5(310)[001]$ tilt W GB by calculating the energetics using a first-principles method. It is found that both the vacancy and SIA are energetically favorable to locate at neighboring sites of the GB, suggesting the vacancy and SIA can easily segregate to the GB region with the segregation energy of 1.53 eV and 7.5 eV, respectively. This can be attributed to the special atomic configuration and large available space of the GB. The effective interaction distance between the GB and the SIA is ~6.19 Å, which is ~2 Å larger than that of the vacancy-GB, indicating the SIA are more preferable to locate at the GB in comparison with the vacancy. Further, the binding energy of di-vacancies in the W GB are much larger than that in bulk W, suggesting that the vacancy energetically prefers to congregate in the GB.

1. Introduction

As an environmentally clean and infinite energy source, nuclear fusion energy is considered as the most effective solution to the energy shortages. Fusion energy is being developed internationally via the International Thermonuclear Experimental Reactor Project, which aims to demonstrate the extended burn of deuterium-tritium (D-T) plasma in a fusion reaction [1]. The application of fusion energy is mainly dependent on the development of the key materials. Tungsten (W) is considered to be the most promising candidate for the plasma-facing material (PFM), because of its high melting temperature, high thermal conductivity and low sputtering erosion [2]. However, during its lifetime, W will be subjected to neutron irradiation, high heat flux and plasma particles bombardment. These circumstances will lead to the deterioration of the W-PFM due to defect formation and displacement damage [3–8].

Defects induced by neutron irradiation in W will lead to material failure [7,8]. Behaviors of point defects play an important role in the degradation of W macroscopic properties [9]. Great efforts have been made to investigate the defect behaviors in W, including hydrogen [10–14], helium [12,15,16], vacancy [17–19] and self-interstitials [19,20]. Grain boundaries (GBs) act as a transition region between two adjacent crystal lattices and thus the crystallographic structure and chemical composition of GBs are distinct from those of the bulk crystal. Nanocrystallized materials contain lots of GBs and interfaces, which are shown to enhance radiation tolerance in extreme environments [21–23]. The GBs and interfaces may serve as effective sinks for defects [11,19,24–26]. Experimentally, much work has been undertaken in the development and preparation of high performance radiation resistance W materials [27,28], which has demonstrated that nanostructured W has a good radiation resistance performance.

In order to understand the effects of GBs on the evolution of irradiation induced defects, a lot of studies have been made to investigate the interaction between the GB and point defects [11,19,24–26]. On the one hand, it has been demonstrated that the GB can emit the interstitials with a low energy barrier to annihilate vacancies in the bulk, which is efficient for self-healing of the radiation-induced damage [22,24]. On the other hand, it is found that the existence of GBs can reduce the formation energy and diffusion barrier of vacancy and self-interstitial atoms (SIA's) [22,24], promoting the recombination rate of Frenkel pairs via the coupling of the individual segregation process of vacancies and SIA near the GB.

Neutron irradiation will produce Frenkel defects (vacancy and SIA), which will further aggregate and form clusters, such as voids

* Corresponding author.
E-mail address: hbzhou@buaa.edu.cn (H.-B. Zhou).

http://dx.doi.org/10.1016/j.nimb.2016.11.040
0168-583X/

and dislocation loops [21]. The combination of Frenkel defects plays an important role in self-healing of radiation damage. Classical atomistic simulations are widely used to study the annihilation process of interstitials and vacancies [22,24,26] within a rather large spatial scale up to billions of atoms and temporal scale up to micro-seconds. Though these classical simulations have advantages on a larger scale and have faster computational simulation speed, they are weak in computational accuracy resulting from the lack of electronic structure information. More accurate statics property results are the basis of the dynamical study of self-healing mechanisms, so the statics study of Frenkel defects using first-principles methods is valuable. In the present work, we have systemically investigated the energetics of Frenkel defects at a W GB using a first-principles method. Our findings give insight into the basic behavior of Frenkel defects in GBs, which will provide a good reference to understand the typical experimental phenomenon related to Frenkel defects. These will be very useful for developing W-PFM for future nuclear fusion reactors.

2. Computational method

We employ a first-principles plane-wave method based on density functional theory (DFT) with generalized gradient approximation (GGA) according to Perdew and Wang [29] using VASP [30,31]. The interaction between ions and electrons is described by the projector augmented wave (PAW) potential based on GGA. The cutoff energy of plane-wave basis set was chosen to be 400 eV. The supercell contains 160 W atoms to simulate the 36.9° Σ5(310)/[001] symmetrical title GB. The GB structure is constructed according to the coincident site lattice (CSL) theory. Specifically, two bcc grains are rotated around the [001] axis by an angle of 36.9°. The mirror-symmetric GB structure used here is quite typical in metallic GBs, which has been widely used for impurity segregation and embrittlement studies [11,32–37]. The calculated equilibrium lattice constant is 3.17 Å for bcc W, in good agreement with the corresponding experimental value of 3.16 Å. The lattice size for the W GB supercell is $10.02 \times 40.87 \times 6.31$ Å^3. In all the calculations, the integrations over the first Brillouin zone were performed by using the special k-point scheme and a $2 \times 1 \times 3$ Monkhorst-Pack k-point mesh [38] with a full relaxation of the atomic positions and volume of the supercell. The energy relaxation iterates until the forces acting on all the atoms are less than 10^{-3} eV Å^{-1}.

3. Results and discussion

3.1. Formation of a single vacancy in the W GB

In order to find the most stable site of a single vacancy in the W GB, the formation energies of a vacancy at eleven different GB sites (see Fig. 1) have been examined. Because of symmetry and periodicity, we only consider a vacancy in the *A* layer. The vacancy formation energy E_V^f is defined as

$$E_V^f = E_{GB+V} - E_{GB} + E_{ref}, \quad (1)$$

where E_{GB+V} and E_{GB} are the total energies of W GB supercell with and without vacancy. E_{ref} is the reference energy for the W atom, which is chosen to be the energy per atom of the W atom in its ground state. Positive vacancy formation energy denotes endothermic, while negative value denotes exothermic.

Fig. 2 shows the vacancy formation energy in the W GB as a function of distance between the vacancy and the GB. It is found that the formation energies of the vacancy are positive for all cases, which indicates that the vacancy formation in the W GB is an endothermic process. Further, the vacancy formation energy at the neighboring sites of the GB (except for the vacancy at the GB plane, S_0) are lower than that in bulk W (~3.11 eV) [39]. This suggests that a vacancy has a tendency to segregate into the neighboring sites of the GB. Besides, the vacancy formation energies increase with increasing the distance between vacancy and the GB (except for the vacancy at the GB plane, S_0). At the most stable site in the GB (S_1), the vacancy formation energy is 1.58 eV. After that, the vacancy formation energy increases to 2.90 eV and 2.64 eV at the distance of 2.14 Å (S_2) and 3.19 Å (S_3), respectively. Beyond this distance, the vacancy formation energy almost converges to a constant ~2.95 eV from ~4.2 Å. Therefore, the effective interaction distance between the GB and the vacancy is approximately 4.2 Å, which is similar to that found in previous studies ~4.7 Å [24]. However, it should be noticed that the vacancy formation energy (~3.18 eV) at the GB plane (S_0 site) is larger than that in bulk W and neighboring sites of the GB. Thus, compared with the GB plane, the neighboring sites of the GB are energetically preferable for the vacancy. It also should be noticed that the vacancy formation energy decreases in the W GB by ~1.53 eV, while a reduction of 0.86 eV was found in previous atomistic simulation studies [24].

To further shed light on the physical origin underlying the stability of a single vacancy in the W GB, the vacancy formation energy is decomposed into two contributions. One is the energy release during lattice relaxation after vacancy formation, the so-called lattice-relaxation contribution. The other is the energy increase during vacancy formation (without atomic relaxation), called the bond-broken contribution. Fig. 2 shows the lattice-relaxation contribution and the bond-broken contribution for the vacancy formation energy in the W GB. Apparently, the bond-broken contribution is much larger than the lattice-relaxation contribution and is 104.2%–136.3% of the vacancy formation energy at different sites in the GB. Besides, the variation tendency of bond-broken contribution is consistent with that of the vacancy formation energy. Therefore, the bond-breaking during vacancy formation is largely responsible for the vacancy formation energy in the GB.

To understand the bond-broken contribution to the vacancy formation energy, the atomic configurations of the GB and bulk W have been investigated. For various vacancy configurations, the vacancy formation energy, the number of first nearest neighbor (1NN) atoms of the vacancy and the shortest distance between the 1NN atom and the vacancy are listed in Table 1. It can be clearly found that the number of 1NN atom for the most stable site (S_1 site) is seven, which is one less than other sites in the GB and bulk W, indicating that the interaction between W(S_1) and its surrounding atoms is weaker than other cases. Further, the shortest distance between 1NN atom and W(S_1) is 2.2 Å, which is much shorter than the optimal W-W distance in the bulk ~2.75 Å. This will also weaken the interaction between W(S_1) and its surrounding atoms. Therefore, the W atom at S_1 is easier to be removed than that at other sites, leading to the decrease of vacancy formation energy.

3.2. Interaction of di-vacancies in W GB

In order to quantify the interaction of di-vacancies, we calculate the binding energy between two vacancies. The first vacancy is set at the most stable site (S_1) in the W GB, while the second one occupies the different neighboring lattice position (S_4 and N_0-N_3, see Fig. 1). The binding energy of di-vacancies can be expressed as

$$E^b_{V_1-V_2} = 2E_{GB+V_1} - E_{GB+V_1+V_2} - E_{GB}, \quad (2)$$

where E_{GB+V_1} is the total energy of the W GB supercell containing one vacancy at S_1. $E_{GB+V_1+V_2}$ is the total energy of the W GB supercell containing di-vacancies. One vacancy is set at S_1 and the other

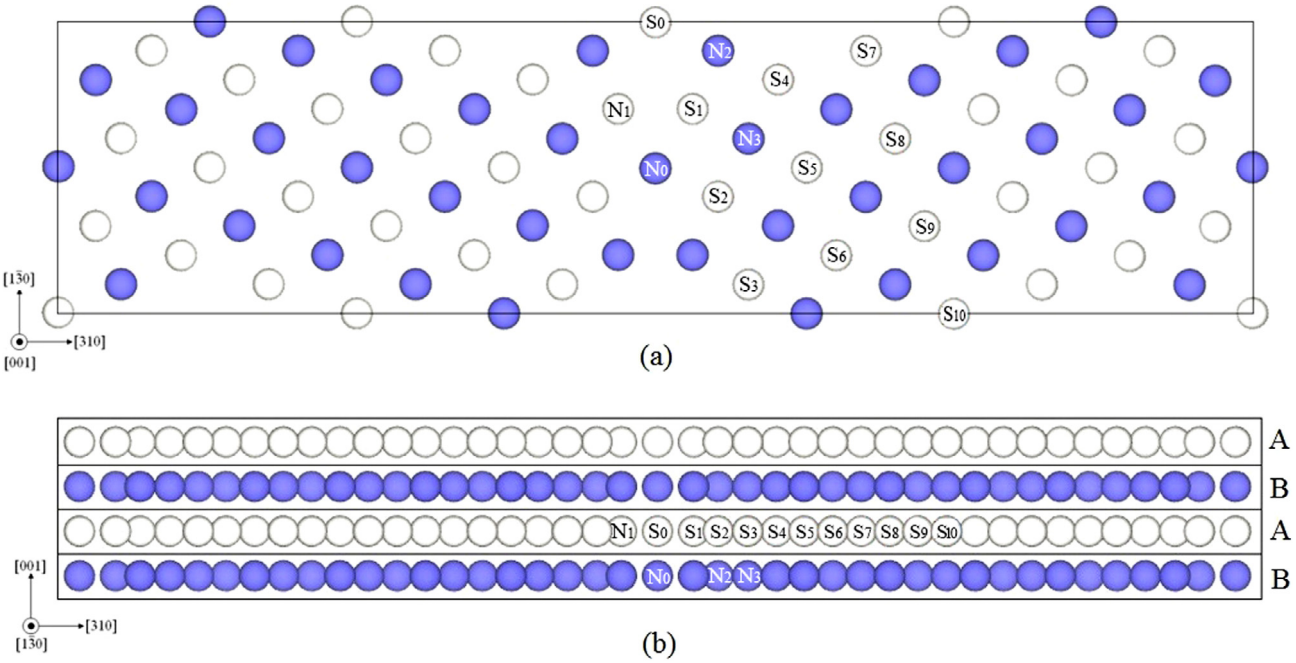

Fig. 1. (a) Top view of the N atom layer of the $\Sigma = 5(3\,1\,0)/[0\,0\,1]$ tilt W GB. (b) Side view of the W GB supercell. Numbers S_0-S_{10} and N_0-N_4 represent different vacancy sites (for later discussion).

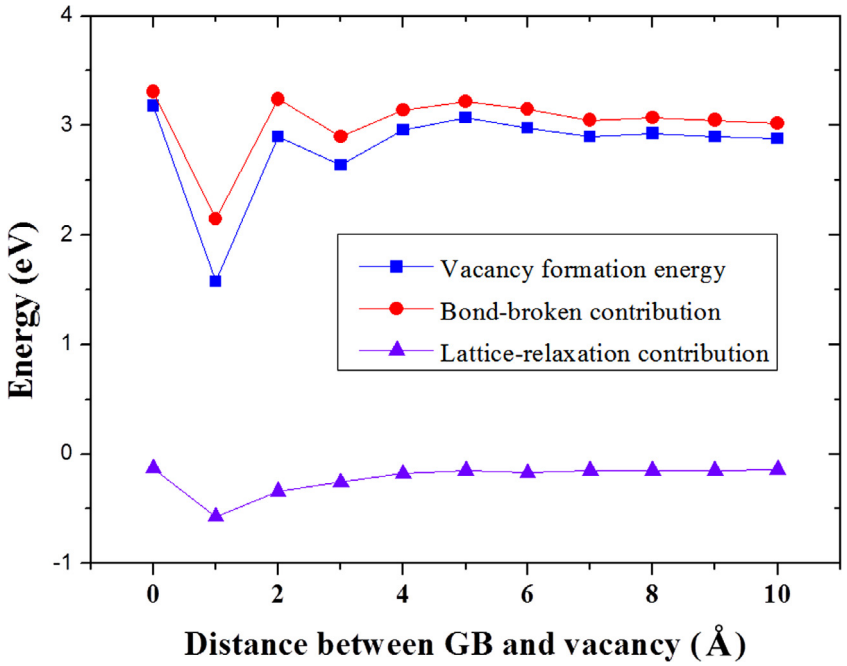

Fig. 2. The formation energy of the vacancy, the lattice-relaxation contribution and the bond-broken contribution in the W GB as a function of distance between the GB and the vacancy. The dashed line presents the V formation energy in bulk W.

Table 1
The vacancy formation energy (in eV), the number of first nearest neighbor (1NN) atoms of the vacancy and the shortest distance (in Å) between the 1NN atom and vacancy in a W GB in comparison with the bulk.

Site	Grain boundary					Bulk	
	S_0	S_1	S_2	S_3	S_4- S_{10}	128-atom	250-atom
Formation energy	3.18	1.58	2.90	2.64	2.88–3.07	3.11	3.15
Number	8	7	8	8	8	8	8
Shortest distance	2.78	2.20	2.42	2.55	2.69–2.71	2.75	2.75

vacancy occupies at other lattice position. A positive value denotes attractive interaction, while a negative one means repulsion. The binding energies of di-vacancies in different configurations are shown in Table 2.

It can be clearly found that the binding energies of di-vacancies are strongly dependent on the configuration. When the second vacancy occupies the N_1 site (corresponding to the first nearest distance ~2.55 Å between two vacancies), the binding energy is −0.56 eV. The most stable di-vacancy configuration occurs at the distance of ~2.70 Å and the binding energy of di-vacancies is 1.16 eV and 0.30 eV for S_1-N_2 and S_1-N_3 with different lattice orientation, respectively, suggesting that there is strong attractive interaction between di-vacancies in the GB. After that, the binding energy decreases to −3.11 eV at the distance of 3.1 Å. Further, it can be found that the binding energy of the most stable di-vacancy configuration in the bulk is a negative value as listed in Table 2, indicating the interaction between vacancies is repulsive. This is in agreement with the previous studies [40]. Therefore, there is a significant difference between di-vacancy behaviors in the W GB and the bulk with the vacancy energetically preferring to get together in the GB.

3.3. Formation of self-interstitial atom in the W GB

Next, we investigate the behavior of the SIA in the W GB. In order to explore the effect of the GB on the stability of the SIA, the formation energies of the SIA are calculated. The formation energy of the SIA can be obtained by

$$E^f_{SIA} = E_{GB+SIA} - E_{GB} - E_{ref}, \quad (3)$$

where E_{GB+SIA} is the total energy of W GB supercell containing one interstitial W atom. According to the previous studies [20,41], the most stable configuration of the SIA in W is the <1 1 1> crowdion. Based on the symmetric analysis of all the <1 1 1> configurations, we find that there are basically two different types of SIA configurations near the W GB, as also reflected in Fig. 3 by the slightly different formation energies. One configuration forms a relatively larger angle between the crowdion direction and the GB plane, the other forms a relative smaller angle. Fig. 3 shows the SIA formation energy near the W GB. The distance is based on the initial positions of the SIA. Generally, the formation energy of the SIA in the W GB can be divided into two regions, namely below and above 6.19 Å. In the former region, the formation energies of the SIA are ~1.93 ± 0.17 eV, which is much lower than that in bulk W ~9.43 eV [34]. This suggests that the SIA can be easily trapped by the W GB. In the latter region, the formation energies of the SIA are ~8.23 ± 0.14 eV, which is slightly lower than that in bulk W. Therefore, the effects of the GB on the formation energy of the SIA should be very small in the latter region. These results suggest that the effective interaction distance between the GB and the SIA is about 6.19 Å. This distance is much longer than the effective

Table 2
The binding energy of di-vacancies with different configurations. The vacancy positions, the distances (Å) and the binding energies (eV) of di-vacancies in a W GB in comparison with the bulk W.

	Grain boundary					Bulk	
First vacancy	S_1					/	/
Second vacancy	N_0	N_1	N_2	N_3	S_4	1NN	2NN
Distance of di-vacancies	2.88	2.55	2.69	2.68	3.1	2.75	3.17
Binding energy	Unstable	−0.56	1.16	0.30	−3.11	−0.21	−0.52

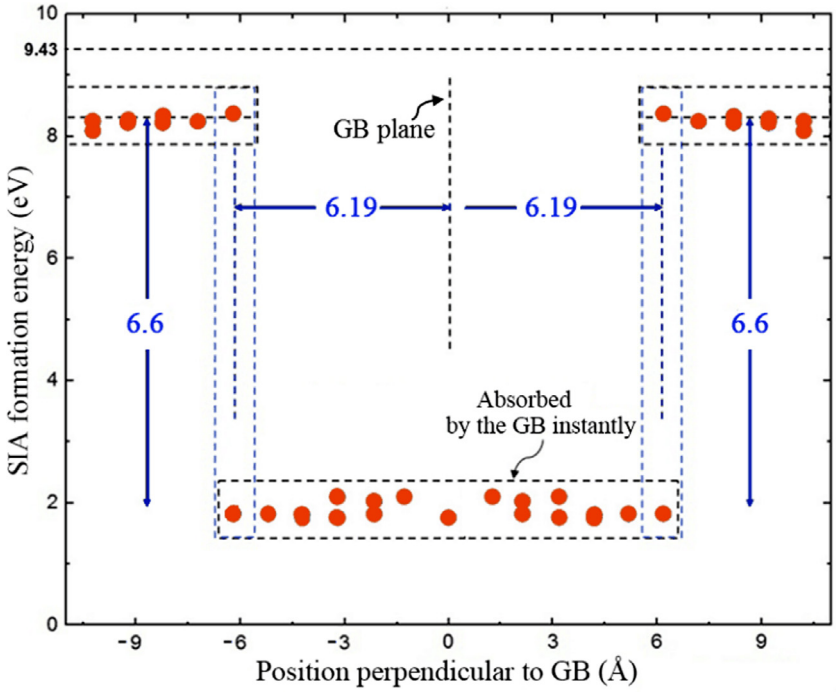

Fig. 3. The formation energy of the SIA from S0 to S10 as a function of the distance from the interstitial to the GB. Note that the distance is based on the initial positions of the SIA. White circles from left to right in the figure are S0 to S10 respectively. The lower dotted marks the S0 to S6 to be absorbed by the grain boundary instantly after relaxation while the upper dotted box marks the S6 to S10 to be absorbed to the middle of two adjacent grain boundaries.

distance between the GB and the vacancy, which is consistent with previous studies [13]. We should note that the values of the SIA formation energy in the GB do not converge to that in the bulk. This discrepancy is primarily due to the presence of residual strain in the cell induced by the relatively small cell size. Therefore, both the GB and the SIA might interact with their periodic images due to their large stress fields.

Further, in order to explore the origin for the SIA formation energy gain in the GB, we also decompose the formation energy into two contributions. One is the energy increase induced by lattice distortion after SIA addition, and called the distortion contribution. The other is the energy increase due to the repulsive interaction between the SIA and its neighboring atoms, called the interatomic repulsion contribution. Here, we consider two different positions (near the GB plane and in the bulk W) for the SIA to explore the effect of the GB on the formation energy of the SIA. When the SIA is near the GB, for example S4, the distortion contribution is 1.82 eV, which is 104% of the SIA formation energy ~1.75 eV. Thus, the distortion contribution is larger than the interatomic repulsion contribution and plays a key role in the SIA formation in the W GB. As to the SIA formation in bulk W, the distortion contribution (8.70 eV) is 92.3% of the formation energy (9.43 eV), which is 6.95 eV larger than that at S4. This suggests that the distortion contribution is also mainly responsible for the reduction of the SIA formation energy in the W GB.

In addition, in order to understand the segregation of the SIA into the W GB, the atomic configurations have been investigated. When the distance between the SIA and the GB is lower than 6.19 Å, the SIA will instantly segregate into the GB via a barrier-free process and then locate at the GB plane. It can be partly understood through the atomic distance between the SIA and its 1NN atom. As shown in Fig. 4, the shortest distance between the SIA and its 1NN atom is 2.31 Å in bulk W, while it is 2.55 Å in the W GB. Further, the number of neighboring atoms (within 3 Å) of the SIA (at GB plane) is seven, while it is eight in bulk W. Therefore, compared with bulk W, the GB provides a larger vacant space for the SIA, which can release the high stress induced by the SIA. Such large available volume will significantly reduce the formation energy of the SIA. Out of the effective interaction region of the GB (within 6.19 Å), the SIA's are stable and must overcome energy barriers jumping from the bulk site to the GB with lower energy.

It should be noted that only one high-angle GB has been considered in the present work. Different GB structures lead to different defect energetics in the GB. Previous atomistic simulations [18,19,24,25] on defect energetics in Fe and W GBs suggest that low-angle GBs have longer absorption length scales (interaction range) than their high-angle counterparts. Using a wide range of GBs with different characteristics, they further demonstrated that the minimum and mean point defect formation energies in the GBs decrease with increasing disorientation angle, GB energy and Σ value [18,25]. The importance of tilt axis and special boundaries such as Σ3(112)/[1–10] twin boundary and Σ5(310)/[001] have also been stressed.

4. Conclusions

In the present work, first-principles calculations have been used to examine point defect energetics near a grain boundary in W. Our results confirm the basic results of previous classical atomistic simulations, but provide improved energetic values for these interactions. We show that the formation energies of the vacancy and SIA near the GB region are lower than that in the bulk W, which can be attributed to the special atomic configuration and large available volume of the GB. This suggests that the GB can serves as an effective sink for irradiation-induced point defects. Further, di-vacancies have a large binding energy in the W GB for some configurations, indicating the GB will facilitate the bonding and aggregation of vacancies. Meanwhile, it should be noticed that there is a difference between vacancy and SIA in the GB. On the one hand, the vacancy formation energy decreases by ~1.53 eV from bulk to the most stable site in the GB, which is approximately 49% of the vacancy formation energy in bulk W. As for the SIA, the reduction is as much as 7.5 eV, which is 80% of the formation energy of the SIA in bulk W. On the other hand, the effective interaction distance between the GB and SIA is about 6.19 Å, which is larger than that between the GB and vacancy ~4.2 Å. Therefore, the GB has a preferential absorption of the SIA compared to the vacancy. In addition, it is well-established that defect energetics also depend significantly on GB character. Here, only one typical GB has been considered. We will further investigate the effect of GB character on the defect energetics in future work.

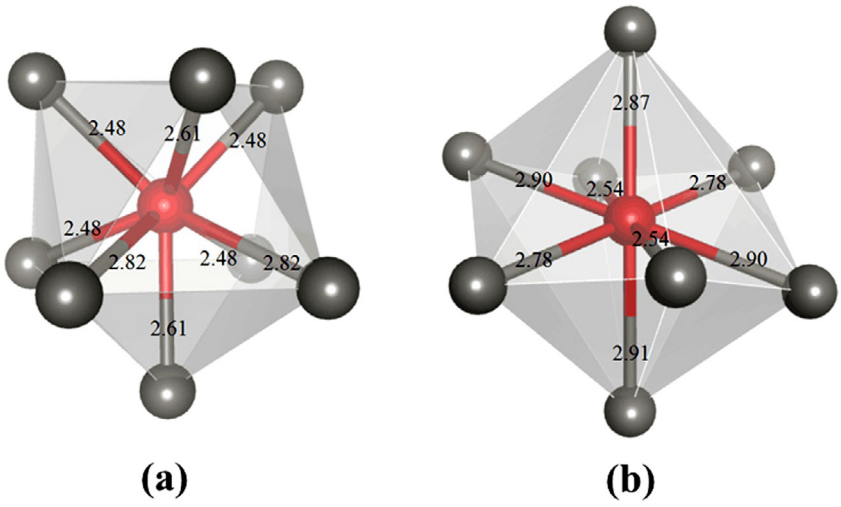

Fig. 4. The atomic configuration of a self-interstitial atom and its neighboring atoms (distance within 3 Å) (a) at the W GB plane and (b) bulk W. The red spheres represent the SIA, while the light gray spheres represent its neighboring W atoms. (For interpretation of the references to colour in this figure legend, the reader is referred to the web version of this article.)

Acknowledgements

This research is supported by the National Magnetic Confinement Fusion Program with Grant No. 2013GB109002, the National Natural Science Foundation of China with Grant No. 11405006, and the National Science Fund for Distinguished Young Scholars through Grant No. 51325103.

References

[1] G. Janeschitz, J. Nucl. Mater. 290–293 (2001) 1–11.
[2] H.T. Lee, A.A. Haasz, J.W. Davis, R.G. Macaulay-Newcombe, J. Nucl. Mater. 360 (2007) 196–207.
[3] M.J. Baldwin, R.P. Doerner, J. Nucl. Mater. 404 (2010) 165–173.
[4] Q. Yang, Y.-W. You, L. Liu, H. Fan, W. Ni, D. Liu, C.S. Liu, G. Benstetter, Y. Wang, Sci. Rep. 5 (2015) 10959.
[5] D.E.J. Armstrong, X. Yi, E.A. Marquis, S.G. Roberts, J. Nucl. Mater. 432 (2013) 428–436.
[6] M. Fukuda, K. Yabuuchi, S. Nogami, A. Hasegawa, T. Tanaka, J. Nucl. Mater. 455 (2014) 460–463.
[7] X. Yi, M.L. Jenkins, M.A. Kirk, S.G. Roberts, Microsc. Microanal. 21 (2015) 117–118.
[8] X. Yi, M.L. Jenkins, M.A. Kirk, Z. Zhou, S.G. Roberts, Acta Mater. 112 (2016) 105–120.
[9] C.-C. Fu, J.D. Torre, F. Willaime, J.-L. Bocquet, A. Barbu, Nat. Mater. 4 (2005) 68–74.
[10] Y.-L. Liu, Y. Zhang, H.-B. Zhou, G.-H. Lu, F. Liu, G.N. Luo, Phys. Rev. B 79 (2009) 172103.
[11] H.-B. Zhou, Y.-L. Liu, S. Jin, Y. Zhang, G.-N. Luo, G.-H. Lu, Nucl. Fusion 50 (2010) 025016.
[12] H.-B. Zhou, Y.-L. Liu, S. Jin, Y. Zhang, G.-N. Luo, G.-H. Lu, Nucl. Fusion 50 (2010) 115010.
[13] H.-B. Zhou, S. Jin, Y. Zhang, G.-H. Lu, F. Liu, Phys. Rev. Lett. 109 (2012) 135502.
[14] H.-B. Zhou, N.K. Momanyi, Y.-H. Li, W. Jiang, X.-C. Li, RSC Adv. 6 (2016) 103622–103631.
[15] H.-B. Zhou, S. Jin, X.-L. Shu, Y. Zhang, G.-H. Lu, F. Liu, EPL (Europhysics Letters). 96 (2011) 66001.
[16] H.-B. Zhou, J.-L. Wang, W. Jiang, G.-H. Lu, J.A. Aguiar, F. Liu, Acta Mater. 119 (2016) 1–8.
[17] H.-B. Zhou, Y.-L. Liu, C. Duan, S. Jin, Y. Zhang, F. Gao, X. Shu, G.-H. Lu, J. Appl. Phys. 109 (2011) 113512.
[18] N. Chen, L.-L. Niu, Y. Zhang, X. Shu, H.-B. Zhou, S. Jin, G. Ran, G.-H. Lu, F. Gao, Sci. Rep. 6 (2016) 36955.
[19] L.-L. Niu, Y. Zhang, X. Shu, S. Jin, H.-B. Zhou, F. Gao, G.-H. Lu, J. Phys.: Condens. Matter 27 (2015) 255007.
[20] L. Chen, Y. Liu, H. Zhou, S. Jin, Y. Zhang, G. Lu, Sci. China Phys., Mechan. Astron. 55 (2012) 614–618.
[21] G. Ackland, Science 327 (2010) 1587–1588.
[22] X.M. Bai, A.F. Voter, R.G. Hoagland, M. Nastasi, B.P. Uberuaga, Science 327 (2010) 1631–1634.
[23] T.D. Shen, S. Feng, M. Tang, J.A. Valdez, Y. Wang, K.E. Sickafus, Appl. Phys. Lett. 90 (2007) 263115.
[24] X. Li, W. Liu, Y. Xu, C.S. Liu, Q.F. Fang, B.C. Pan, J.-L. Chen, G.-N. Luo, Z. Wang, Nucl. Fusion 53 (2013) 123014.
[25] M.A. Tschopp, K.N. Solanki, F. Gao, X. Sun, M.A. Khaleel, M.F. Horstemeyer, Phys. Rev. B 85 (2012) 064108.
[26] X. Li, W. Liu, Y. Xu, C.S. Liu, B.C. Pan, Y. Liang, Q.F. Fang, J.-L. Chen, G.N. Luo, G.-H. Lu, Z. Wang, Acta Mater. 109 (2016) 115–127.
[27] H. Kurishita, S. Matsuo, H. Arakawa, T. Sakamoto, S. Kobayashi, K. Nakai, H. Okano, H. Watanabe, N. Yoshida, Y. Torikai, Y. Hatano, T. Takida, M. Kato, A. Ikegaya, Y. Ueda, M. Hatakeyama, T. Shikama, Phys. Scr. 2014 (2014) 014032.
[28] C. Gonzalez, M. Panizo-Laiz, N. Gordillo, C.L. Guerrero, E. Tejado, F. Munnik, P. Piaggi, E. Bringa, R. Iglesias, J.M. Perlado, R. Gonzalez-Arrabal, Nucl. Fusion 55 (2015) 113009.
[29] J. Perdew, J. Chevary, S. Vosko, K. Jackson, M. Pederson, D. Singh, C. Fiolhais, Phys. Rev. B 46 (1992) 6671–6687.
[30] G. Kresse, J. Furthmüller, Phys. Rev. B 54 (1996) 11169–11186.
[31] G. Kresse, J. Furthmüller, Comput. Mater. Sci. 6 (1996) 15–50.
[32] L. Zhang, C.-C. Fu, G.-H. Lu, Phys. Rev. B 87 (2013) 134107.
[33] M. Všianská, M. Šob, Prog. Mater Sci. 56 (2011) 817–840.
[34] M. Všianská, M. Šob, Phys. Rev. B 84 (2011) 014418.
[35] M. Černý, P. Šesták, P. Řehák, M. Všianská, M. Šob, Mater. Sci. Eng. A 669 (2016) 218–225.
[36] R. Wu, A.J. Freeman, G. Olson, Science 265 (1994) 376–380.
[37] M. Yamaguchi, M. Shiga, H. Kaburaki, Science 307 (2005) 393–397.
[38] H.J. Monkhorst, J.D. Pack, Phys. Rev. B 13 (1976) 5188–5192.
[39] Y.-L. Liu, Y. Zhang, G.N. Luo, G.-H. Lu, J. Nucl. Mater. 390–391 (2009) 1032–1034.
[40] C.S. Becquart, C. Domain, Nucl. Instr. Methods Phys. Res. B 255 (2007) 23–26.
[41] P.M. Derlet, D. Nguyen-Manh, S.L. Dudarev, Phys. Rev. B 76 (2007) 054107.